Acta Crystallographica Section F
Structural Biology and Crystallization Communications
ISSN 1744-3091

A model for 3-methyladenine recognition by 3-methyladenine DNA glycosylase I (TAG) from *Staphylococcus aureus*

Xiaofeng Zhu, Xuan Yan, Lester G. Carter, Huanting Liu, Shirley Graham, Peter J. Coote and James Naismith*

The BSRC, University of St Andrews, North Haugh, St Andrews KY16 9ST, Scotland

Correspondence e-mail: naismith@st-and.ac.uk

Received 29 March 2012
Accepted 15 April 2012

PDB References: 3-methyladenine DNA glycosylase I–3-MeA complex, 4aia; Y16F mutant, 4ai5.

The removal of chemically damaged DNA bases such as 3-methyladenine (3-MeA) is an essential process in all living organisms and is catalyzed by the enzyme 3-MeA DNA glycosylase I. A key question is how the enzyme selectively recognizes the alkylated 3-MeA over the much more abundant adenine. The crystal structures of native and Y16F-mutant 3-MeA DNA glycosylase I from *Staphylococcus aureus* in complex with 3-MeA are reported to 1.8 and 2.2 Å resolution, respectively. Isothermal titration calorimetry shows that protonation of 3-MeA decreases its binding affinity, confirming previous fluorescence studies that show that charge–charge recognition is not critical for the selection of 3-MeA over adenine. It is hypothesized that the hydrogen-bonding pattern of Glu38 and Tyr16 of 3-MeA DNA glycosylase I with a particular tautomer unique to 3-MeA contributes to recognition and selection.

1. Introduction

Bacterial 3-methyladenine DNA glycosylase I (TAG; Forsyth *et al.*, 2002; Ji *et al.*, 2001) is ubiquitous in eubacteria (Supplementary Fig. S1[1]; Drohat *et al.*, 2002) but shows no sequence or structural similarity to mammalian 3-methyladenine DNA glycosylase (AAG; Lau *et al.*, 2000). TAG belongs to the alkylpurine DNA glycosylase superfamily and hydrolyzes the N9–C1′ glycosylic bond between a 3-methyladenosine (3-MeA) nucleobase lesion and the deoxyribose ring (Riazuddin & Lindahl, 1978; Bjelland *et al.*, 1993; Fig. 1*a*). 3-Methylation of adenine does not influence base pairing (Sedgwick *et al.*, 2007); rather, the methyl group blocks replication by interfering with the interactions of DNA polymerase (Sedgwick *et al.*, 2007; Engelward *et al.*, 1996). Like the 8-oxoguanylate DNA glycosylases MutM and hOGG1 (Banerjee *et al.*, 2005, 2006; Banerjee & Verdine, 2006; Blainey *et al.*, 2006), TAG is thought to slide along the duplex until it encounters a lesion. TAG binds flipped-out 3-MeA and then cleaves the damaged base from the ribose. TAG from *Staphylococcus aureus* shares around 40% amino-acid sequence identity with the structurally characterized TAG enzymes from *Salmonella typhi* (Metz *et al.*, 2007) and *Escherichia coli* (Drohat *et al.*, 2002). The crystal structure of the *S. typhi* enzyme complexed with 3-MeA and abasic DNA (Metz *et al.*, 2007) and an NMR structure of the *E. coli* enzyme complexed with 3-MeA (Cao *et al.*, 2003) have been reported. Two absolutely conserved residues, Tyr16 and Glu38, were identified to form hydrogen bonds with 3-MeA and Trp46 stacks with 3-MeA (Cao *et al.*, 2003; Metz *et al.*, 2007). The methyl group does not appear to make extensive contacts. The crystal structure of the apo *S. aureus* enzyme has been reported (Oke *et al.*, 2010). We wished to probe the basis of the discrimination between adenine and 3-MeA in the *S. aureus* enzyme.

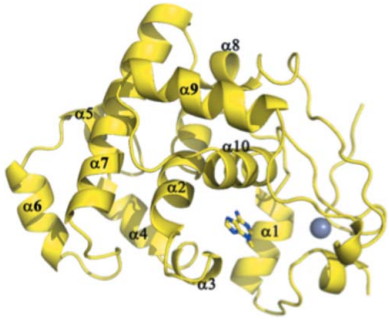

[1] Supplementary material has been deposited in the IUCr electronic archive (Reference: GX5204).

2. Materials and methods

2.1. Protein production

Native and mutant protein were purified as described by Oke *et al.* (2010). Y16F and E38Q mutations were introduced using QuikChange (Stratagene); primers are listed in Table 1.

Fluorescence binding measurements were performed as described by Cao *et al.* (2003) and Drohat *et al.* (2002). 2 µ*M* TAG was titrated with 10–650 µ*M* 3-MeA or adenine in 20 m*M* phosphate buffer pH 7.8 and 5.8; Figs. 2*a* and 2*b*). Isothermal titration calorimetry (ITC) experiments were carried out using a VP-ITC device (MicroCal) in the same buffer. 5 m*M* 3-MeA or 1.5 m*M* adenine solution was injected at 298 K into a sample cell containing ∼1.4 ml protein solution at 30–40 µ*M*. Each titration consisted of a first 1 µl injection followed by up to 25 subsequent 10 µl injections or 48 subsequent 5 µl injections of the ligand as indicated. Calorimetric data were analyzed using the MicroCal *ORIGIN* software, fixing the stoichiometry as $N = 1$ (Figs. 2*c* and 2*d*; Supplementary Table S1).

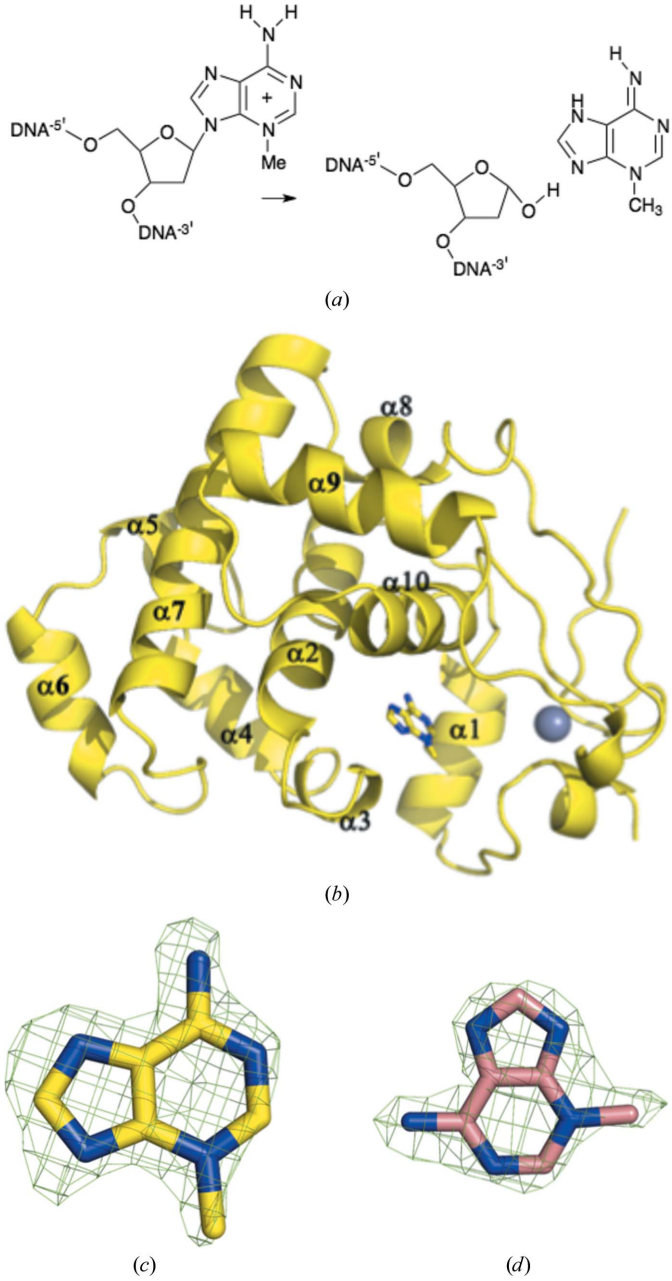

Figure 1
(*a*) The reaction catalyzed by TAG. (*b*) TAG is mainly α-helical; a structural zinc ion (grey sphere) is a found in all homologues of the enzyme. 3-MeA is shown in stick representation, with C atoms coloured yellow, N atoms coloured blue and O atoms coloured red. (*c*) Difference $F_o - F_c$ electron density contoured at 3σ for 3-MeA in the active site of TAG. (*d*) Difference $F_o - F_c$ electron density contoured at 3σ for 3-MeA in the active site of Y16F-mutant TAG; C atoms are coloured pink. 3-MeA binds in a different orientation in the Y16F mutant.

Table 1
Macromolecule-production information.

The following primers were used to create the mutations: Y16F, 5′-GTACTAAAGATCCAGTCTACTTAAAC**TTT**CATGATCATGTATGGG-3′ and 5′-CCCATACATGATCATG**AAA**GTTTAAGTAGACTGGATCTTTAGTAC-3′; E38Q, 5′-GCAAGGCATTGTTTAAACTTTTAGCATTA**CAG**TCACAACATGCTGGG-3′ and 5′-CCCAGCATGTTGTGA**CTG**TAATGCTAAAAGTTTAAACAATGCCTTGC-3′. Mutation sites are shown in bold.

Source organism	*S. aureus* strain MSSA476
Expression vector	pHis-TEV
Expression host	*E. coli*
Complete amino-acid sequence of the construct produced	GAMNECAFGTKDPVYLNYHDHVWGQPLYDSKALFKLLALESQHAGLSWLTILKKKEAYEEAFYDFEPEKVAQMTAQDIDR LMTFPNIVHHRKKLEAIVNQAQGYLKIEQAYGSFSKFLWSYVNGKPKDLQYEHASDRITVDDTATQLSKDLKQYGFKFLGPVTVFSFLEAAGLYDAHLKDCPSKPKHN

Table 2
Data-collection and processing statistics.

Values in parentheses are for the last shell.

Protein	Native, 3-MeA complex	Y16F, 3-MeA complex
Diffraction source	ESRF beamline ID14-2	Rotating anode
Wavelength (Å)	0.933	1.54
Temperature (K)	100	100
Detector	ADSC Quantum 4 CCD	Saturn CCD
Crystal-to-detector distance (mm)	203	55
Rotation range per image (°)	0.2	0.5
Total rotation range (°)	108	180
Exposure time per image (s)	5	5
Space group	*C*2	*C*2
Unit-cell parameters		
a, *b*, *c* (Å)	73.00, 78.59, 179.81	72.3, 78.8, 179.3
α, β, γ (°)	90, 90.56, 90	90, 90.5, 90
Mosaicity (°)	0.3	0.56
Resolution range (Å)	29.60–1.80 (1.85–1.80)	50–2.2 (2.28–2.20)
Total No. of reflections	341926	118143
No. of unique reflections	92544 (5876)	47714 (3209)
Completeness (%)	98.4 (91.6)	95.5 (89.1)
Redundancy	3.7 (3.1)	2.6 (2.3)
$\langle I/\sigma(I)\rangle$	17.50 (3.9)	28.2 (10.9)
$R_{r.i.m.}$†	0.059 (0.292)	0.04 (0.11)
Overall *B* factor from Wilson plot (Å^2)	18	24.2

† Estimated $R_{r.i.m.} = R_{merge}[N/(N-1)]^{1/2}$, where N is the data multiplicity.

2.2. Crystallization

Sitting-drop vapour-diffusion crystallization trials (1 µl protein solution plus 1 µl precipitant solution) were set up using a Cartesian Honeybee nanodrop crystallization robot which was integrated in a Hamilton-Thermo Rhombix system. The 3-MeA complexes of native and Y16F TAG were obtained by incubating TAG with 10 m*M* 3-MeA for 6 h before crystallization at 277 K. The complex crystals grew using a precipitant solution consisting of 0.1 *M* Tris–HCl pH 8.5, 1.8 *M* ammonium sulfate, 0.2 *M* Li_2SO_4 at 293 K as thin plates and grew to full size (0.2 × 0.2 × < 0.05 mm) in two to three weeks. Cryoprotectant solution was made by supplementing the crystallization precipitant solution with 20% glycerol. Crystals were mounted

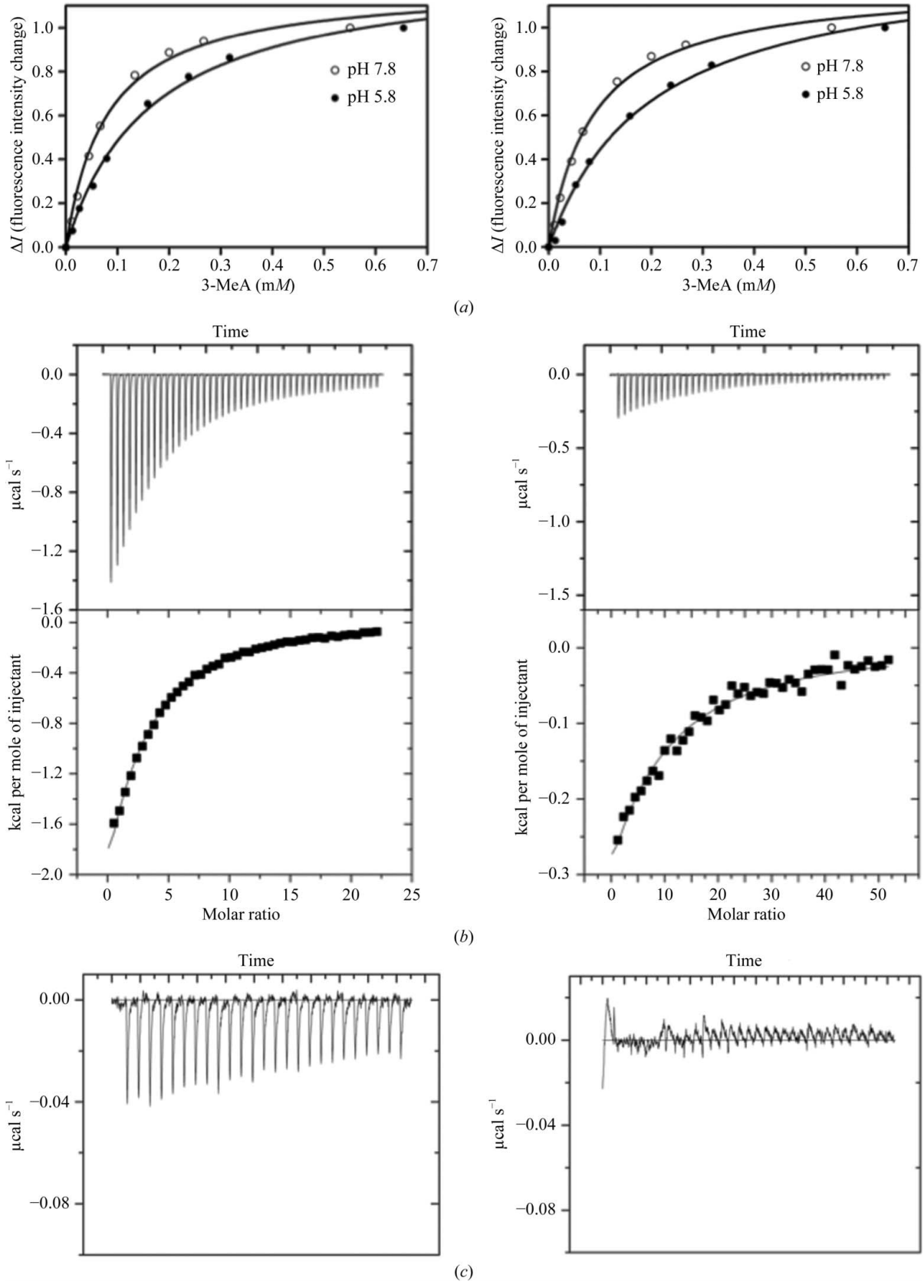

Figure 2
(*a*) Measurement of the binding of 3-MeA to *S. aureus* TAG using intrinsic fluorescence quenching at pH 5.8 (K_d = 165 μ*M*) and pH 7.8 (K_d = 78 μ*M*); the results are similar to those previously reported for the *E. coli* enzyme (Cao *et al.*, 2003). (*b*) Fluorescence quenching of 3-MeA with E38Q-mutant *S. aureus* TAG at pH 5.8 and 7.8. The small reduction in the binding constant was inconsistent with structural and previous functional data (Cao *et al.*, 2003). This indicated that the fluorescence was unreliable for the *S. aureus* enzyme. (*c*) ITC measurement of the binding of 3-MeA to *S. aureus* TAG at pH 7.8 (K_d = 220 μ*M*) and pH 5.8 (K_d = 470 μ*M*). Adenosine does not bind. (*d*) ITC measurement of the binding of 3-MeA to Y16F-mutant (K_d = 1.2 m*M*; left) and E38Q-mutant (no binding; right) *S. aureus* TAG at pH 7.8. 1 cal = 4.186 kJ.

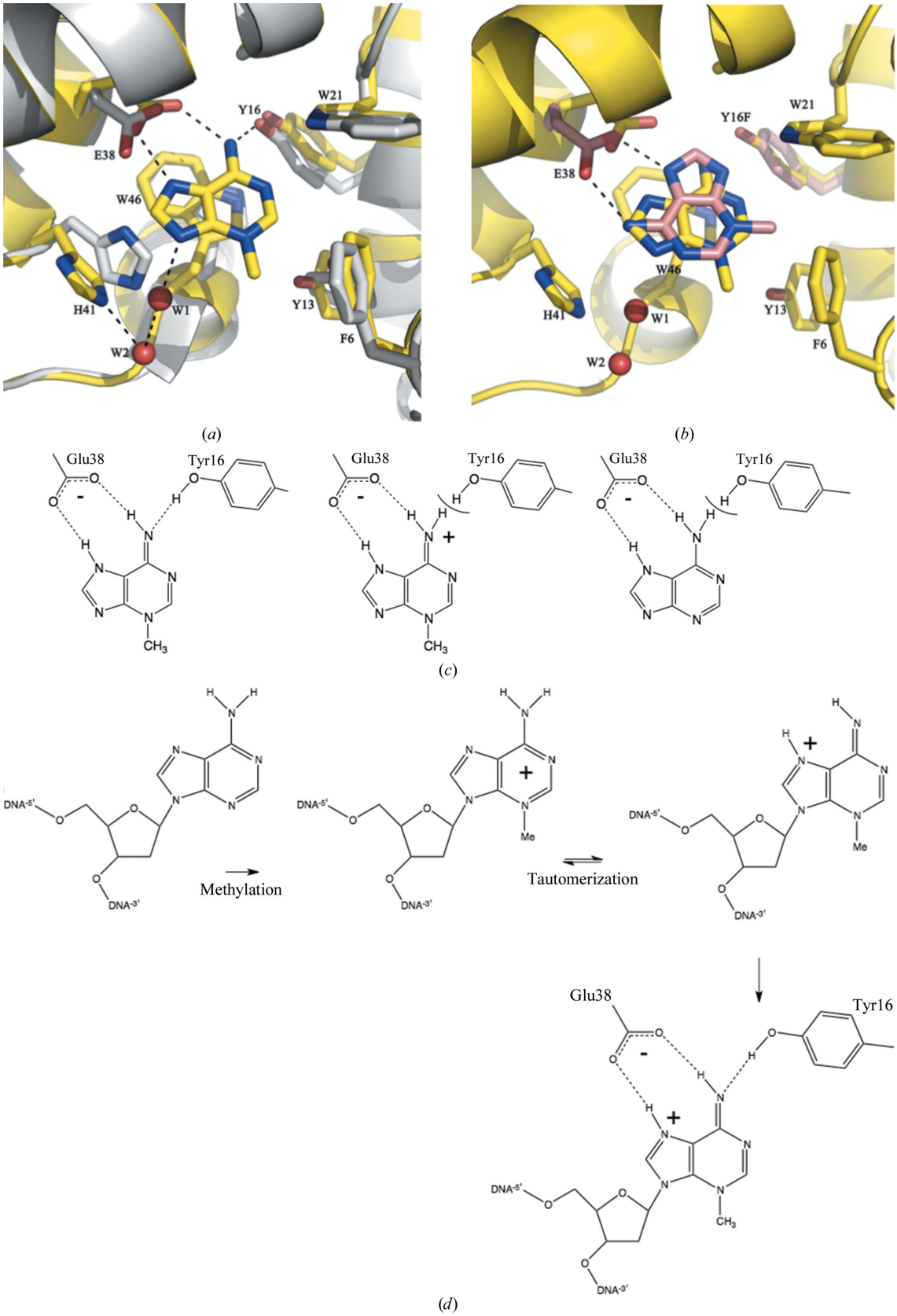

Figure 3
(*a*) Structure of the 3-MeA–TAG complex (C atoms, yellow; N atoms, blue; O atoms, red) showing the key interactions. The apo structure is shown with C atoms in white. (*b*) Structure of the 3-MeA–Y16F TAG complex (C atoms shown in pink); the 3-MeA ring adopts a different orientation in the mutant. The 3-MeA in the native protein is also shown. (*c*) The most common tautomer of 3-MeA could be recognized by a specific hydrogen-bond arrangement of Tyr16 and Glu38. The predominant tautomer of protonated 3-MeA and adenosine would not match this hydrogen-bonding arrangement. (*d*) DNA damage leads to formation of the positively charged tautomer that is optimal for recognition by TAG; in addition, the highly electron-deficient ring would interact favourably with the TAG active site.

in Hampton Research cryoloops and rapidly cooled to 100 K prior to data collection.

2.3. Data collection and processing

Data for the native TAG–3-MeA complex were collected from a single crystal using 0.2° oscillations at a wavelength of 0.933 Å (ESRF beamline ID14-2) and were reduced using *XDS* (Kabsch, 2010). Data were collected from a single crystal of the Y16F TAG–3-MeA complex using an in-house Rigaku MicroMax-007 HF rotating-anode generator and Saturn 944 CCD detector. Data were reduced using *HKL*-2000 (Otwinowski & Minor, 1997) and *POINTLESS* (Evans, 2006; Potterton *et al.*, 2003; Winn *et al.*, 2011). Full details are given in Table 2. The E38Q mutant was also crystallized, but as no 3-MeA was located in the active site the structure is not described here; however, the structure has been deposited (PDB entry 4ai4).

2.4. Structure solution and refinement

The structures were solved with *Phaser* (McCoy *et al.*, 2007) using the native apo structure (Oke *et al.*, 2010; PDB entry 2jg6) as a search model. As the complex crystals grew in a different space group to the native crystals, a new free set of reflections was assigned for refinement. All structures were refined with *REFMAC* v.5.6.0117 (Murshudov *et al.*, 2011); manual intervention employed *Coot* (Emsley & Cowtan, 2004). 3-MeA was added to the models when the $F_o - F_c$ density was clear (Figs. 1*c* and 1*d*). *MolProbity* (Chen *et al.*, 2010) was used for structure validation and Ramachandran analysis. TLS parameters were used in refinement. TLS groups were assigned using the *TLSMD* server (Painter & Merritt, 2006). Details of the refinement are given in Table 3.

Table 3
Structure refinement.

Values in parentheses are for the last shell.

Protein	Native, 3-MeA complex (PDB entry 4aia)	Y16F, 3-MeA complex (PDB entry 4ai5)
Resolution range (Å)	28.19–1.80 (1.847–1.800)	179.29–2.22 (2.276–2.218)
Completeness (%)	98.2	95.3
σ cutoff	0	0
No. of reflections, working set	87884 (5568)	45350 (3043)
No. of reflections, test set	4654 (308)	2364 (166)
Final R_{cryst}	0.179 (0.233)	0.183 (0.193)
Final R_{free}	0.218 (0.289)	0.216 (0.244)
No. of non-H atoms		
Protein	7598	7602
Ion	25	25
Ligand	55	55
Water	927	486
Total	8605	8168
R.m.s. deviations		
Bonds (Å)	0.009	0.015
Angles (°)	1.189	1.550
Average *B* factors (Å^2)		
Protein	22.2	21.7
Ion	29.9	29.2
Ligand	15.4	17.3
Water	25.5	22.1
Ramachandran plot		
Favoured regions (%)	98.5	98.4
Additionally allowed (%)	1.4	1.5

3. Results and discussion

The structure of the *S. aureus* TAG–3-MeA complex was determined to 1.8 Å resolution and that of the Y16F TAG–3-MeA complex to 2.22 Å resolution. The structure of the native 3-MeA complex is very similar to the crystal structure of the *S. typhi* TAG–3-MeA–abasic DNA complex (Metz *et al.*, 2007) and the NMR structure of the *E. coli* TAG–3-MeA complex (Cao *et al.*, 2003). Relative to apo TAG (Oke *et al.*, 2010), Glu38 has rotated to make 2.7 Å contacts with the exocyclic N atom and N7 of 3-MeA. Tyr16 moves to make a 2.8 Å contact with the exocyclic N atom of 3-MeA (Fig. 3*a*). Trp46 stacks with the bound purine ring of 3-MeA, while Phe6, Tyr13 and Tyr21 make edge-on contacts. His41 rotates 80° to create space for 3-MeA to bind. The Y16F-mutant complex revealed that 3-MeA adopts a different orientation, although it preserves a bidentate hydrogen bond to Glu38 and a stacking interaction with Trp46 (Fig. 3*b*). This conformation is unlikely to be physiologically relevant, as it would require a very different orientation of the DNA to that observed in the *S. typhi* complex (Metz *et al.*, 2007). Using a fluorescence assay, we measured 3-MeA binding (Fig. 2*a*), obtaining a similar result at pH 7.8 (K_d = 78 µ*M*) to that for the *E. coli* enzyme at pH 7.5 (K_d = 42 µ*M*; Cao *et al.*, 2003). However, the assay is flawed for the *S. aureus* enzyme as the E38Q mutant gave the same result as for the native protein (Fig. 2*b*), which is physically unreasonable. ITC (Figs. 2*c* and 2*d*) showed clear differences between the native and mutant *S. aureus* enzymes (Y16F, K_d = 1.2 m*M*; E38Q, no binding) and gave K_d values of 220 µ*M* at pH 7.8 and 471 µ*M* at pH 5.8 for the native enzyme. We did not detect adenine binding.

3-Methyldeoxyadenosine is positively charged in DNA, whilst deoxyadenosine is neutral; simple charge–charge recognition was therefore the original explanation for the specificity of TAG (Labahn *et al.*, 1996; Lau *et al.*, 2000; Hollis *et al.*, 2000). However, it has been shown that *E. coli* TAG binds 3-MeA but not adenine and binds protonated 3-MeA (pH 5.7) more weakly than neutral 3-MeA (pH 7.5) (Cao *et al.*, 2003; Drohat *et al.*, 2002), establishing that charge–charge recognition is not the sole explanation (Cao *et al.*, 2003). We suggest that a particular hydrogen-bond pattern contributes to the selection of a specific but favoured (Sharma & Lee, 2002) neutral tautomer of 3-MeA (Fig. 3*c*) that is not available to adenosine (Fig. 3*c*) and that is disfavoured for protonated 3-MeA (Fig. 3*c*). Our hypothesis implies that there is an energetic penalty in reorganizing the hydrogen-bond network around Tyr16 to avoid a van der Waals clash (Fig. 3*c*). In DNA, 3-methyldeoxyadenosine can adopt a tautomer that has the same hydrogen arrangement as neutral 3-MeA and has positive charge (Fig. 3*d*), which is favoured at the active site (Metz *et al.*, 2007). A clash of H atoms was observed between the amide of His136 and the amino group of adenine in human AAG and is used to preferentially select the damaged purine base (O'Brien & Ellenberger, 2004). Higher resolution data or neutron diffraction are required to further test the hypothesis for the TAG enzyme.

The work was funded by the BBSRC SPoRT initiative (BB_BBS/B/14426).

References

Banerjee, A., Santos, W. L. & Verdine, G. L. (2006). *Science*, **311**, 1153–1157.
Banerjee, A. & Verdine, G. L. (2006). *Proc. Natl Acad. Sci. USA*, **103**, 15020–15025.
Banerjee, A., Yang, W., Karplus, M. & Verdine, G. L. (2005). *Nature (London)*, **434**, 612–618.
Bjelland, S., Bjørås, M. & Seeberg, E. (1993). *Nucleic Acids Res.* **21**, 2045–2049.
Blainey, P. C., van Oijen, A. M., Banerjee, A., Verdine, G. L. & Xie, X. S. (2006). *Proc. Natl Acad. Sci. USA*, **103**, 5752–5757.
Cao, C., Kwon, K., Jiang, Y. L., Drohat, A. C. & Stivers, J. T. (2003). *J. Biol. Chem.* **278**, 48012–48020.
Chen, V. B., Arendall, W. B., Headd, J. J., Keedy, D. A., Immormino, R. M., Kapral, G. J., Murray, L. W., Richardson, J. S. & Richardson, D. C. (2010). *Acta Cryst.* D**66**, 12–21.

Drohat, A. C., Kwon, K., Krosky, D. J. & Stivers, J. T. (2002). *Nature Struct. Biol.* **9**, 659–664.
Emsley, P. & Cowtan, K. (2004). *Acta Cryst.* D**60**, 2126–2132.
Engelward, B. P., Dreslin, A., Christensen, J., Huszar, D., Kurahara, C. & Samson, L. (1996). *EMBO J.* **15**, 945–952.
Evans, P. (2006). *Acta Cryst.* D**62**, 72–82.
Forsyth, R. A. *et al.* (2002). *Mol. Microbiol.* **43**, 1387–1400.
Hollis, T., Ichikawa, Y. & Ellenberger, T. (2000). *EMBO J.* **19**, 758–766.
Ji, Y., Zhang, B., Van Horn, S. F., Warren, P., Woodnutt, G., Burnham, M. K. & Rosenberg, M. (2001). *Science*, **293**, 2266–2269.
Kabsch, W. (2010). *Acta Cryst.* D**66**, 125–132.
Labahn, J., Schärer, O. D., Long, A., Ezaz-Nikpay, K., Verdine, G. L. & Ellenberger, T. E. (1996). *Cell*, **86**, 321–329.
Lau, A. Y., Wyatt, M. D., Glassner, B. J., Samson, L. D. & Ellenberger, T. (2000). *Proc. Natl Acad. Sci. USA*, **97**, 13573–13578.
McCoy, A. J., Grosse-Kunstleve, R. W., Adams, P. D., Winn, M. D., Storoni, L. C. & Read, R. J. (2007). *J. Appl. Cryst.* **40**, 658–674.
Metz, A. H., Hollis, T. & Eichman, B. F. (2007). *EMBO J.* **26**, 2411–2420.
Murshudov, G. N., Skubák, P., Lebedev, A. A., Pannu, N. S., Steiner, R. A., Nicholls, R. A., Winn, M. D., Long, F. & Vagin, A. A. (2011). *Acta Cryst.* D**67**, 355–367.
O'Brien, P. J. & Ellenberger, T. (2004). *J. Biol. Chem.* **279**, 9750–9757.
Oke, M. *et al.* (2010). *J. Struct. Funct. Genomics*, **11**, 167–180.
Otwinowski, Z. & Minor, W. (1997). *Methods Enzymol.* **276**, 307–326.
Painter, J. & Merritt, E. A. (2006). *J. Appl. Cryst.* **39**, 109–111.
Potterton, E., Briggs, P., Turkenburg, M. & Dodson, E. (2003). *Acta Cryst.* D**59**, 1131–1137.
Riazuddin, S. & Lindahl, T. (1978). *Biochemistry*, **17**, 2110–2118.
Sedgwick, B., Bates, P. A., Paik, J., Jacobs, S. C. & Lindahl, T. (2007). *DNA Repair*, **6**, 429–442.
Sharma, S. & Lee, J. K. (2002). *J. Org. Chem.* **67**, 8360–8365.
Winn, M. D. *et al.* (2011). *Acta Cryst.* D**67**, 235–242.